Dissociable neural circuits for encoding and retrieval of object locations during active navigation in humans

Oliver Baumann *, Edgar Chan, Jason B. Mattingley

The University of Queensland, Queensland Brain Institute & School of Psychology, St Lucia, Queensland, 4072, Australia

ARTICLE INFO

ABSTRACT

Several cortical and subcortical circuits have been implicated in object location memory and navigation. Uncertainty remains, however, about which neural circuits are involved in the distinct processes of encoding and retrieval during active navigation through three-dimensional space. We used functional magnetic resonance imaging (fMRI) to measure neural responses as participants learned the location of a single target object relative to a small set of landmarks. Following a delay, the target was removed and participants were required to navigate back to its original position. The relative and absolute locations of landmarks and the target object were changed on every trial, so that participants had to learn a novel arrangement for each spatial scene. At encoding, greater activity within the right hippocampus and the parahippocampal gyrus bilaterally predicted more accurate navigation to the hidden target object in the retrieval phase. By contrast, during the retrieval phase, more accurate performance was associated with increased activity in the left hippocampus and the striatum bilaterally. Dividing participants into good and poor navigators, based upon behavioural performance, revealed greater striatal activity in good navigators during retrieval, perhaps reflecting superior procedural learning in these individuals. By contrast, the poor navigators showed stronger left hippocampal activity, suggesting reliance on a less effective verbal or symbolic code by this group. Our findings suggest separate neural substrates for the encoding and retrieval stages of object location memory during active navigation, which are further modulated by participants' overall navigational ability.

© 2009 Elsevier Inc. All rights reserved.

Introduction

As humans navigate, they acquire knowledge about their environment, such as the spatial layout of salient landmarks based upon visual, proprioceptive, and kinaesthetic inputs. This information is encoded and stored in memory, allowing us to find our way back to a desired location within the same environment. In humans, three brain regions have been proposed to play a key role in the process of learning the layout of large-scale environments through navigational experience: the *hippocampus* (e.g., Doeller et al., 2008; Ekstrom et al., 2003; Ekstrom and Bookheimer, 2007; Grön et al., 2000; Wolbers et al., 2007), the *parahippocampus* (e.g., Ekstrom and Bookheimer, 2007; Epstein, 2008; Janzen and van Tourennout, 2004), and the *striatum* (e.g., Bohbot et al., 2004; Doeller et al., 2008; Orban et al., 2006). Although all three regions have been implicated in spatial navigation, it remains unclear how each contributes to the distinct processes of encoding and retrieval during the learning of novel spatial arrays. Several previous fMRI studies have investigated memory retrieval of object locations, while others have sought to identify the functional anatomy of three-dimensional spatial memory as a whole, without

distinguishing between the distinct stages of encoding and retrieval. The neural bases of these processes have received considerable attention in cognitive domains such as verbal working memory and episodic memory (e.g., Ludowig et al., 2008; Schacter and Wagner, 1999). In the area of human spatial navigation, however, no previous fMRI study has examined patterns of neural activity associated with encoding and retrieval processes within the context of a single behavioural task.

In the present study, we sought to identify the neural circuits that underlie the distinct processes of encoding and retrieval during landmark-based navigation. We used event-related fMRI to measure neural responses as participants navigated a virtual environment. It has been shown that cognitive maps built up in virtual environments are comparable to those acquired in the real environment (Ruddle et al., 1997) and that spatial knowledge acquired in virtual environments can be transferred to the real world (Richardson et al., 1999). The principal limitation of studies that have used realistic virtual environments, such as towns or cities, is that the number, location, and relative salience of paths and landmarks cannot be adequately quantified or controlled. To overcome this problem, we employed a sparse virtual environment that consisted of an infinite, textured plain containing three cylindrical landmarks and a distinctive, pyramid-shaped target object. In the initial encoding phase of each trial, participants were required to navigate to and encode the

* Corresponding author. Fax: +61 7 3346 6301.
 E-mail address: o.baumann@uq.edu.au (O. Baumann).

location of the target object. After a short delay, participants re-entered the arena from one of four different positions and were required to navigate back to the remembered location of the target, which had been removed from the display. We sought to identify brain regions whose activity patterns predicted navigation performance, with the aim of determining the neural circuits underlying the formation and retrieval of landmark-based spatial representations. We also divided participants into 'good' and 'poor' navigators, based upon their behavioural performance, to determine whether activity in specific brain regions predicts participants' overall navigational ability.

Method

Participants

Seventeen right-handed, healthy male volunteers (mean age = 31.6 years, SD = 7.4) with normal or corrected-to-normal vision gave written informed consent to participate in the study, which was approved by the University of Queensland Ethics Committee.

Task and stimuli

We used the Blender open source 3D content creation suite (The Blender Foundation, Amsterdam, the Netherlands) to create a virtual environment and administer the navigation task. Participants moved through the virtual arena by means of a joystick held in their right hand. The arena consisted of an infinite plain with a pebble-like texture covering the ground to enhance its 3D quality. It contained four visual objects, with three serving as landmarks and one as the target (Fig. 1a). The landmarks were cylinders (red, green, and blue) with a virtual height of 2.2 m and a diameter of 1 m. The target was a yellow pyramid with a virtual height and width of 50 cm. The pyramid had a virtual 'light beacon', which projected vertically from the apex, to allow its position to be determined when occluded by the landmarks. In the *encoding phase*, participants were instructed to remember the relative location of the target object with respect to the three landmarks, which constituted the only reliable points of reference. On each trial, they were asked to navigate to the target and press a button on the joystick to indicate when they arrived there. Participants were trained to complete the encoding phase within a time limit of 8 seconds. The encoding phase was followed by a short delay period (3.5 seconds) in which the display remained blank. In the subsequent *retrieval phase*, participants re-entered the arena, either from the same location as in the encoding phase or from a different location (shifted by 90°, 180°, or 270°, with equal probability). During retrieval, the landmarks appeared in their original locations, but the target was now absent. Participants were required to navigate back to the remembered location of the target, and to press a button on the joystick when they arrived there. The retrieval phase had a time limit of 7 seconds. Following completion of the retrieval phase, the display remained blank for 5 seconds before participants commenced the next trial (see Fig. 1b). The locations of the landmarks and target object within the arena were altered on every trial to ensure that a completely new spatial layout had to be learned on each occasion.

In a baseline condition, participants completed trials in which the target object *remained visible* during the retrieval phase. The baseline condition therefore replicated the pattern of visual stimulation and the motor demands of the experimental task but did not explicitly require participants to encode or retrieve the target location during active navigation. Participants received a cue prior to each trial to indicate whether they were about to undertake the experimental or baseline task. The study consisted of 56 experimental trials and 56 baseline trials, which were randomly intermingled in four separate runs of
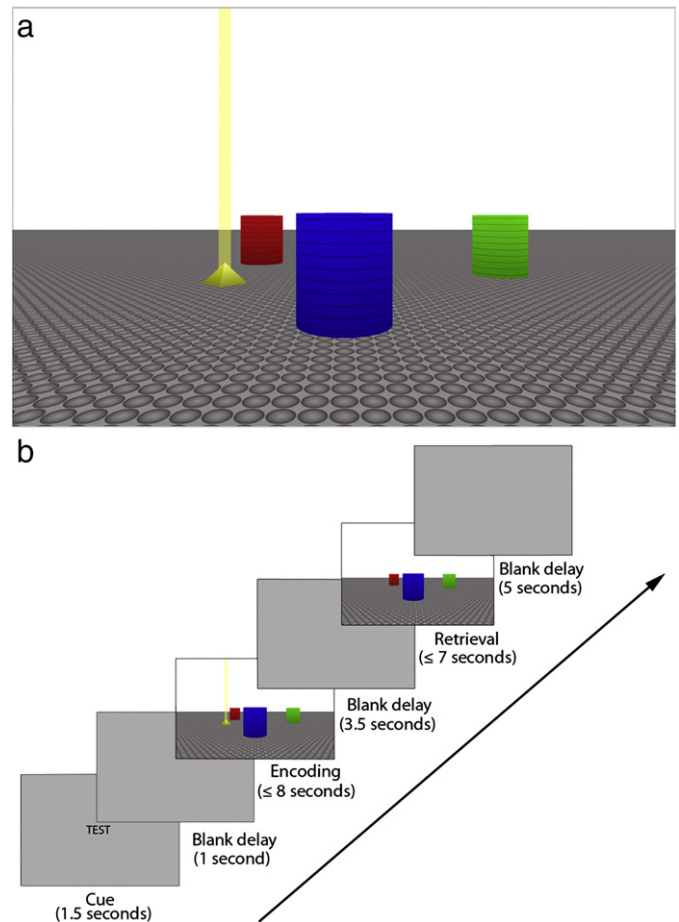
Fig. 1. Schematic of the virtual environment used in the navigation task. (a) Example display of the virtual environment during the encoding phase of an experimental trial. Landmarks are shown in red, green, and blue. The target is shown in yellow, with a virtual light beacon projecting vertically from its apex. (b) Sequence of events in a typical experimental trial. Participants entered the environment and navigated to the target before pressing a button on the joystick to indicate when they reached its location. The encoding phase was followed by a short delay period in which the display remained blank. In the subsequent retrieval phase, participants re-entered the arena from either the same location as in the encoding phase (25% of trials) or from a different location (shifted by 90°, 180°, or 270°; 75% of trials). They were required to navigate to the location of the target, which was now absent from the display, and to indicate via the joystick when they had arrived there. The next trial commenced after a further delay of 5 seconds.

equal length. Before the experimental session, all participants performed extensive training to enable them to navigate effectively within the brief encoding and retrieval periods. We recorded the participants' absolute metric error (defined as the distance in virtual metres between the target's location and the location indicated by the participant) as a measure of their performance. We also recorded other behavioural variables related to participants' movements within the virtual environment, including their speed of movement (defined as the rate of change in position, measured in virtual metres per second), duration (defined as the amount of time required by participants to complete the encoding and retrieval phases of the task), and unsigned rotation (defined as the cumulative sum of the participants' angular motion within the virtual environment; this variable effectively describes the amount of "turning" a participant engages in).

MRI acquisition

Brain images were acquired on a 1.5-T MR scanner (Sonata; Siemens, Erlangen, Germany) with a standard head coil. For the

functional data thirty-two axial slices (slice thickness, 3.5 mm) were acquired in an interleaved order, using a gradient echo echo-planar T2*-sensitive sequence (repetition time, 2.48 s; echo time, 40 ms; flip angle, 90°; matrix, 64×64; field of view, 230×230 mm; voxel size, 3.59×3.59×3.5 mm; image size, 131,072 voxels). On average 243 (SD = 10) volumes per session were acquired for each participant. We also acquired a T1-weighted structural MPRAGE scan. A liquid crystal display projector (1024×768 resolution) back-projected the virtual environment onto a screen positioned at the end of the scanner bed. Participants lay on their backs within the bore of the magnet and viewed the stimuli comfortably via a 45° angled mirror that reflected the images displayed on the screen. The distance to the screen was 265 cm (15 cm from eyes to mirror) and the visible part of the screen encompassed approximately 21°×11° of visual angle (98×50 cm). To minimize head movement, all participants were stabilized with tightly packed foam padding surrounding the head. Since the hippocampus and adjacent brain areas are typical 'dropout' regions in MRI due to inhomogeneities near air/tissue borders, we used optimal EPI parameters to image these brain regions, as reported by Weiskopf et al. (2006).

Image processing and statistical analysis of fMRI data

Image processing and statistical analyses were performed using SPM5 (Wellcome Department of Imaging Neuroscience, UCL, London, UK). Functional data volumes were slice-time corrected and realigned to the first volume. A T2*-weighted mean image of the unsmoothed images was coregistered with the corresponding anatomical T1-weighted image from the same individual. The individual T1-image was used to derive the transformation parameters for the stereotaxic space using the SPM5 template (Montreal Neurological Institute (MNI) Template), which was then applied to the individual coregistered EPI images. The voxel sizes of the normalised images were 2 mm³. Images were then smoothed with an 8-mm full-width half-maximum (FWHM) isotropic Gaussian kernel, in accordance with previous studies that focused their analyses on hippocampal, parahippocampal and striatal structures (Doeller et al., 2008; Epstein et al., 2007; Wolbers et al., 2007). At the single-participant level, we applied a high-pass filter to remove baseline drifts. Encoding and retrieval periods for the experimental trials and their equivalents within the baseline condition were modeled separately as boxcar functions convolved with a hemodynamic response function (HRF), with predicted responses always covering the entire period. Consistent with recent literature in the field (Doeller et al., 2008; Epstein et al., 2007; Wolbers et al., 2007), we sought to increase the sensitivity of our analyses by focusing on a small set of selected areas of the brain that have been shown to be critical for active visual navigation. Our region-of-interest (ROI) analyses targeted the hippocampus, parahippocampal gyrus and striatum, separately within the left and right hemispheres.

To assess within-participant performance effects on a trial-by-trial basis, we added regressors in which the HRFs of the regressors resembling the encoding and retrieval periods were parametrically modulated (linearly scaled) by absolute metric error on each trial, following Wolbers et al. (2007). Specific effects were tested with appropriate linear contrasts of the parameter estimates, and the corresponding contrast images were subsequently entered into a random effects analysis. Main effects of object location encoding and retrieval, as well as performance-related activation, were assessed with single-sample *t*-tests. In a separate analysis, we also modelled activations within the regions of interest related to participants' movements in the virtual environment. To do this, we included parametric modulations of the regressors for the encoding and retrieval periods by speed and unsigned rotation.

In addition to examining the effects of within-participant performance variability, we also investigated the relationship between blood oxygenation level-dependent (BOLD) responses and *between*-participant variability. To identify the neural foundations of between-participant variability, we implemented a median split among participants based on the average absolute metric error. We then conducted *t*-tests using individual contrast images reflecting mean activation during encoding and retrieval periods (one image per participant). We also conducted a multiple regression analysis, using the average metric error as a predictor of BOLD activity.

Results

Behavioural data

The average duration, movement speed and extent of rotational movement for the encoding and retrieval phases, and the equivalent variables for the baseline condition, are shown in Fig. 2. Participants were significantly faster in the retrieval condition than in the corresponding baseline condition (paired *t*-test, $P<0.05$). There were no significant differences between the experimental and the corresponding baseline conditions for the other behavioural parameters. None of these behavioural variables correlated significantly with absolute metric errors ($P>0.05$), nor was there any significant correlation between accuracy in locating the target and trial number ($P>0.05$), indicating that behavioural performance remained consistent over the course of the experiment. Participants performed no better – either in terms of navigational accuracy or response speed – for trials in which they entered the virtual arena from identical versus different locations in the encoding and retrieval phases. A median split of participants into two groups based on their absolute error yielded an average error for the good navigators ($N = 8$) of 2.20 virtual metres (SD = 0.15), and an average error for the poor navigators of 3.13 virtual metres (SD = 0.5). There were no significant differences between the two groups for the other behavioural parameters (duration, speed, or unsigned rotation, *t*-tests, $P>0.05$).
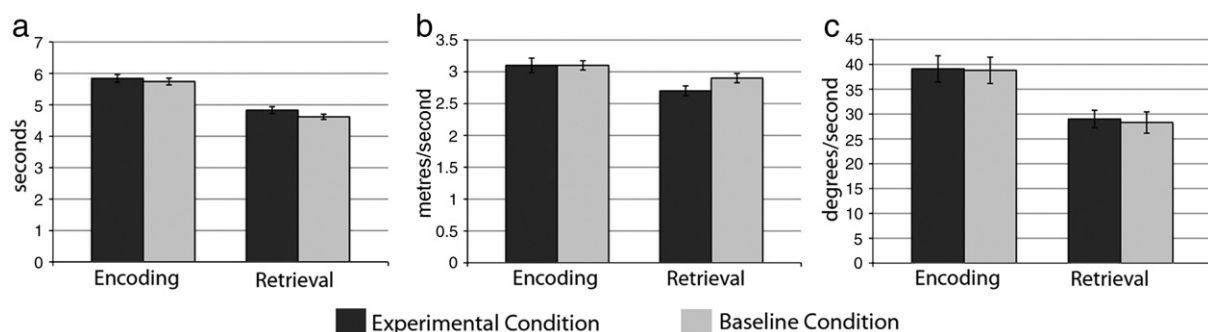
Fig. 2. Mean behavioural performance (±1 standard error) during encoding and retrieval phases of the navigation task, plotted separately for the experimental and baseline conditions. (a) Duration. (b) Speed. (c) Unsigned rotation.

After completion of the fMRI experiment we asked participants to rate on a 10-point scale how often they used a verbal strategy (e.g., inner speech) to remember the target's location (1 = 'never' and 10 = 'always'). We predicted that use of a verbal strategy would reduce accuracy in the task because verbal codes cannot effectively capture the fine-grained metric relationships between landmarks and the target object. Participants' average rating on this measure was 7.94. We conducted a correlation analysis to determine whether participants' ratings correlated with average absolute error in locating the target object during the retrieval phase. Participants who were more inclined to use a verbal strategy during the navigation task also made larger errors in locating the object (Pearson product-moment correlation, $df = 14$, $r = 0.81$, $P < 0.01$).

Brain imaging data

Brain imaging data were analysed separately for the encoding and retrieval phases of the navigation task. As outlined in the Method, we defined a priori ROIs for structures known to be involved in spatial learning and navigation. These were the hippocampus (e.g., Doeller et al., 2008; Ekstrom et al., 2003; Ekstrom and Bookheimer, 2007; Grön et al., 2000; Janzen et al., 2008; Wolbers et al., 2007), the parahippocampus (e.g., Aguirre et al., 1996; Aminoff et al., 2007; Ekstrom and Bookheimer, 2007; Epstein 2008; Janzen and van Tourennout, 2004; Maguire et al., 1998), and the striatum (e.g., Bohbot et al., 2004; Doeller et al., 2008; Orban et al., 2006). All ROIs were defined separately for the left and right hemispheres using the AAL atlas (Tzourio-Mazoyer et al., 2002). Voxels were counted as active if they surpassed a statistical threshold of $P = 0.05$ (corrected for multiple comparisons). Although our primary focus was on these three key regions, we also performed exploratory whole-brain analyses to identify regions that were differentially activated during the navigation task compared with the baseline (visuomotor control) task (height threshold $P = 0.00001$; extent threshold $P = 0.05$, corrected for multiple comparisons).

Main effect of memory-guided navigation

We first contrasted activity during the experimental task with activity during the baseline condition, separately for the encoding and retrieval periods, to identify overall activation attributable to the different stages of memory-guided navigation. For the *encoding phase*, the whole-brain analysis yielded significant activations in the visual cortex, inferior and superior parietal lobules, precuneus, cerebellum and several frontal cortical regions. Within the targeted ROIs, there was a significant response within bilateral hippocampus, bilateral striatum, and the right parahippocampus (see Tables 1a and 1b and Fig. 3). Analysis of the whole-brain during the *retrieval phase* revealed significant activations in the visual cortex, inferior and superior parietal lobules, precuneus, cerebellum, cingulate cortex, thalamus, supramarginal gyrus, striatum, parahippocampus, and several frontal cortical regions. During the retrieval phase, there was no significant activity within the hippocampus at either the ROI or whole-brain level.

Within-participant performance effects

The overall comparison between the experimental and baseline conditions presumably identified regions that might also be involved in aspects of visuospatial processing that are not directly related to successful memory-guided navigation. To determine which areas are specifically involved in the spatial memory process, we included absolute metric errors, a measure of trial-by-trial accuracy in locating

Table 1a
Summary of fMRI findings for the contrast of experimental and baseline conditions during the encoding phase.

Region	Hemisphere	Brodmann area	MNI coordinates			T values/z values of maxima (cluster size in number of voxels)
			X	Y	Z	
Whole brain						
CingG/SFG/MedFG	L/R	6/32	−6	8	54	9.91/5.53 (183)
IPL/precuneus/SPL	R	7/40	32	−60	56	9.14/5.34 (515)
MOG/SOG/cuneus/precuneus	L	18/19/31	−20	−78	18	8.76/5.23 (188)
PrecG/MFG	R	6	40	−6	50	8.66/5.20 (121)
MOG/MTG	L	19	−44	−80	14	8.41/5.13 (22)
PrecG/MFG	L	6	−48	−6	52	7.85/4.96 (77)
IPL	L	40	−44	−52	52	7.74/4.92 (137)
PostCing/LingG/cuneus	R	18/23/30	4	−64	4	7.72/4.92 (111)
MFG/SFG	L	6	−30	−4	58	7.68/4.90 (64)
Cerebellum (posterior lobe)	R	–	34	−48	−40	7.64/4.89 (19)
Cerebellum (posterior lobe)	L	–	−38	−44	−42	7.57/4.87 (17)
Precuneus/SPL	L	7	−32	−64	54	7.53/4.85 (82)
MOG/cuneus/precuneus	R	19	26	−80	22	7.34/4.79 (113)
Precuneus	L	7	−14	−80	54	7.13/4.72 (16)
Cerebellum (vermis/posterior lobe)	L/R	–	6	−70	−24	7.08/4.70 (39)
IFG	L	9	−48	6	32	6.42/4.46 (8)
LingG/cuneus	L	18	−10	−76	0	6.19/4.36 (10)
Cerebellum (posterior lobe)	L	–	−40	−66	−30	6.17/4.35 (8)
ROI						
Striatum (caudate)	L	–	−4	18	2	7.27/4.77 (68)
Hippocampus (posterior)	L	–	−24	−30	−4	6.74/4.58 (57)
Striatum (caudate)	R	–	6	18	4	5.51/4.07 (15)
Hippocampus (posterior)	R	–	20	−34	2	5.48/4.05 (42)
Striatum (caudate)	R	–	18	26	−2	5.22/3.93 (16)
Striatum (putamen)	L	–	−20	14	6	4.92/3.78 (104)
Parahippocampus	R	–	34	−40	−12	4.74/3.69 (35)

Spatial coordinates, anatomical locations and cluster size of the local maxima in the group analysis, showing significant activations ($P ≤ 0.05$, corrected for multiple comparisons) for the contrast (a) encoding minus baseline, and (b) retrieval minus baseline.
Abbreviations: AntCing = anterior cingulate, CinG = cingulate gyrus, IFG = inferior frontal gyrus, IPL = inferior parietal lobule, ITG = inferior temporal gyrus, L = left hemisphere, LingG = Lingual Gyrus, MedFG = medial frontal gyrus, MFG = middle frontal gyrus, MOG = middle occipital gyrus, MTG = middle temporal gyrus, PostCing = posterior cingulate, PrecG = precentral gyrus, R = right hemisphere, SFG = superior frontal gyrus, SOG = superior occipital gyrus, SPL = superior parietal lobule.
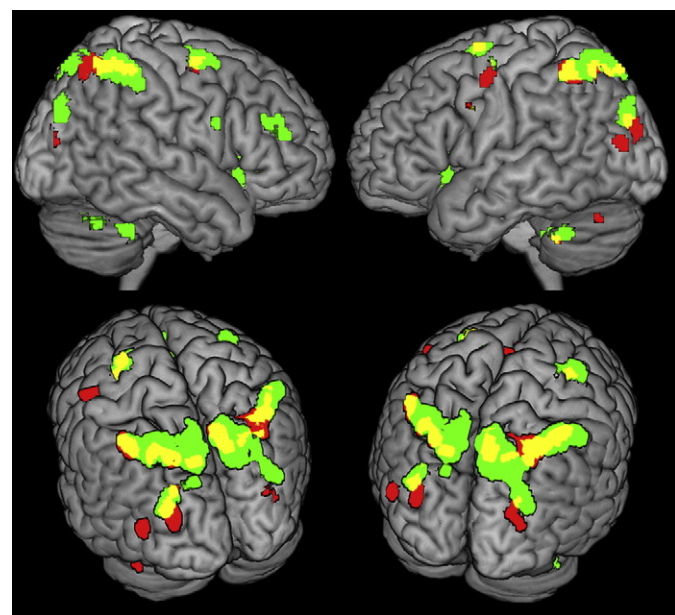
Table 1b
Summary of fMRI findings for the contrast of the experimental and baseline conditions during the retrieval phase.

Region	Hemisphere	Brodmann area	MNI coordinates			T values/z values of maxima (cluster size in number of voxels)
			X	Y	Z	
Whole brain						
SOG/IPL/precuneus/SPL	R	7/40	38	−52	54	15.02/6.51 (2073)
IFG/putamen/caudate/thalamus	R	13/45/47	32	24	−2	14.94/6.50 (864)
IFG/insula	L	13/45/47	−34	24	−2	12.37/6.06 (263)
IPL/precuneus/SPL	L	7/40	−34	−54	48	11.67/5.93 (1114)
Cerebellum (anterior and posterior lobe)	L	–	−34	−50	−36	11.02/5.79 (466)
MedFG/SFG/CingG/	L/R	6/8/32	4	14	52	10.67/5.71 (430)
MFG	R	6	30	−6	54	10.27/5.62 (455)
MFG/SFG	L	6	−28	0	66	10.24/5.61 (300)
SOG/precuneus/cuneus	L	7/19	−28	−78	32	9.58/5.45 (282)
MFG	R	10	38	36	22	9.57/5.45 (86)
Thalamus	L	–	−12	−14	2	9.49/5.43 (51)
Cerebellum (anterior/posterior lobe)	R	–	38	−44	−36	9.45/5.42 (251)
Caudate/putamen	L	–	16	4	12	9.27/5.37 (334)
Fusiform gyrus	R	19	28	−42	−10	8.64/5.20 (33)
Cerebellum (anterior lobe)	L/R	–	4	−52	−24	7.80/4.94 (37)
AntCing/CingG	R	32	10	24	30	7.63/4.89 (25)
PostCing/cuneus/precuneus	L	18/31	−14	−70	14	7.36/4.80 (20)
Precuneus	L	7/19	−14	−78	38	7.24/4.76 (20)
PrecG/IFG	L	9	−48	4	30	7.10/4.71 (13)
Cuneus	R	17/18/23	12	−76	12	6.90/4.63 (27)
LingG	L	18	−12	−88	−8	6.90/4.63 (27)
Cerebellum (posterior lobe)	L	–	−8	−74	−28	6.76/4.58 (25)
IFG	R	44	54	8	24	6.60/4.52 (11)
Cerebellum (posterior lobe)	R	–	8	−70	−28	6.57/4.51 (17)
ROI						
Striatum (caudate)	R	–	16	4	12	9.27/5.37 (715)
Striatum (caudate)	L	–	−14	2	14	9.15/5.34 (809)
Parahippocampal gyrus	R	–	28	−42	−8	7.91/4.98 (83)
Parahippocampal gyrus	L	–	−28	−44	−8	6.28/4.40 (22)

Spatial coordinates, anatomical locations and cluster size of the local maxima in the group analysis, showing significant activations ($P \leq 0.05$, corrected for multiple comparisons) for the contrast (a) encoding minus baseline, and (b) retrieval minus baseline.
Abbreviations: AntCing = anterior cingulate, CinG = cingulate gyrus, IFG = inferior frontal gyrus, IPL = inferior parietal lobule, ITG = inferior temporal gyrus, L = left hemisphere, LingG = Lingual Gyrus, MedFG = medial frontal gyrus, MFG = middle frontal gyrus, MOG = middle occipital gyrus, MTG = middle temporal gyrus, PostCing = posterior cingulate, PrecG = precentral gyrus, R = right hemisphere, SFG = superior frontal gyrus, SOG = superior occipital gyrus, SPL = superior parietal lobule.

Fig. 3. Three-dimensional rendered MR images showing mean BOLD activity from the whole-brain analysis of experimental minus baseline conditions. Red shading represents activity during the encoding phase; green shading represents activity during the retrieval phase; yellow shading indicates overlaps. Activation maps are overlaid onto a rendered MNI-normalized template. Activated voxels buried within sulci are projected onto the cortical surface.

the target object, as a parametric modulation regressor in the general linear model.

At encoding, greater activity within the right hippocampus predicted more accurate navigation to the (hidden) target object in the later retrieval phase (see Fig. 4 and Table 2). By contrast, during the retrieval phase, more accurate performance was associated with increased activity in the left hippocampus (Fig. 5 and Table 2). We also found that participants' accuracy in locating the target during retrieval was predicted by increased activity within the parahippocampal gyrus bilaterally at encoding. By contrast, there was no such relationship between performance and parahippocampal activity during the retrieval phase. An inverse pattern emerged for the striatum. During encoding, this area showed no performance-related effects, whereas during retrieval, activity in both the left and right striatum was a strong predictor of task performance.

Given that the different sizes of the predefined ROIs can induce a bias in the form of different statistical thresholds, we re-analysed the parametric modulation of BOLD activity by absolute metric errors using an uncorrected height threshold of $P = 0.001$ for the whole brain. This analysis did not reveal any significant voxels, using a threshold of $P = 0.05$, beyond those already identified in the ROI approach, thus confirming the anatomical specificity of the results. Further analyses failed to reveal any significant correlations between brain activity and participants' speed of movement or rotation. Performance-dependent activation patterns therefore cannot be attributed merely to differences in motor responses. Since absolute metric errors did not correlate with time elapsed since the onset of the experiment (trial number) the performance-dependent activation patterns also cannot be attributed to declining performance over the course of the experiment.

Fig. 4. MR brain slices depicting within-participants performance effects for the encoding phase. Parametric analysis revealed a negative correlation between BOLD activation during encoding of the object location and absolute metric error on a trial-by-trial basis in three regions. (a) Left parahippocampus (−28, −44, −8). (b) Right parahippocampus (30, −26, −16). (c) Right hippocampus (36, −22, −8).

Between-participant performance effects

Recent fMRI studies (Epstein et al., 2005; Hartley et al., 2003; Janzen et al., 2008) have shown differential neural activity for good and poor navigators. Epstein et al. (2005) showed stronger fMRI repetition effects for spatial scenes in good versus poor navigators, suggesting more efficient scene processing in individuals with superior navigational skills. Hartley et al. (2003) found greater activity in the right hippocampus for good versus poor navigators, in a task that required participants to find novel paths between locations. By contrast, Janzen et al. (2008) detected increased activity in bilateral hippocampus for objects encountered during the initial stages of a navigation task than for those encountered toward the end, but only in good navigators. It remains unknown, however, whether the representation of spatially relevant objects varies as a function of navigational ability across individuals.
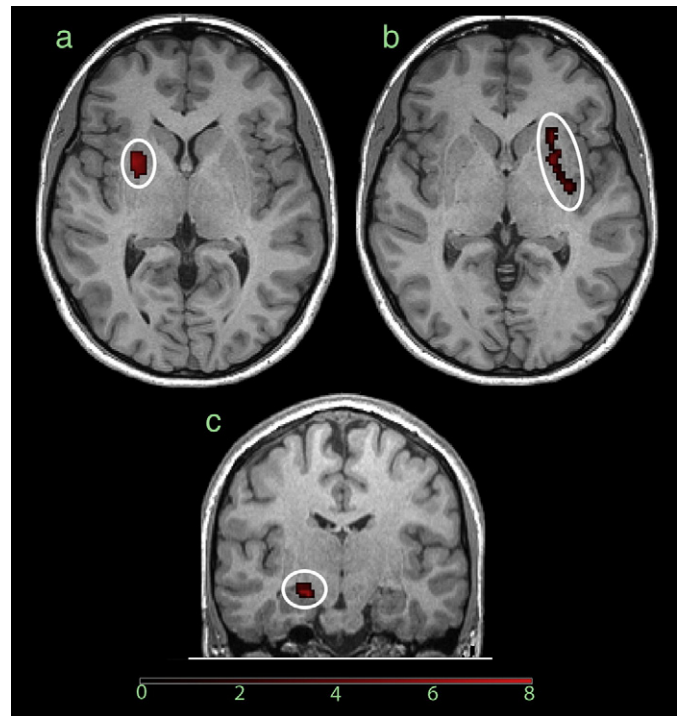
Fig. 5. MR brain slices depicting within-participants performance effects for the retrieval phase. Parametric analysis revealed a negative correlation between BOLD activation during retrieval of the object location and absolute metric error on a trial-by-trial basis in three regions. (a) Left striatum (putamen; −30, 6, 0). (b) Right striatum (putamen; 24, 6, 0). (c) Left hippocampus (−22, −10, −18).

To elucidate the brain regions involved in navigational skill in our task, we examined the relationship between participants' average behavioural performance and their pattern of brain activity. A multiple regression analysis, using the average metric error as a predictor of BOLD activity, did not reveal a significant linear relationship between accuracy and neural responses. We then separated participants using a median split, based on average absolute metric error. A t-test on neural responses in the two groups revealed that, during the encoding phase, there was significantly greater activity in the right medial and posterior parietal cortex (Brodmann area 7) in the good navigators than in the poor navigators (Table 3a). During the retrieval phase, the good navigators also showed significantly more activity bilaterally in the parietal cortex, cerebellum, frontal regions (Fig. 6 and Table 3b) and striatum (Figs. 7a and b and 8a and b), parietal cortex, cerebellum, and frontal regions. The most extensive frontal activations were located bilaterally in the inferior frontal cortex (Brodmann area 47), a region that has been associated with both spatial and non-spatial memory tasks (e.g., Courtney et al., 1997;

Table 2
Summary of fMRI findings for the negative parametric modulation of BOLD activity with absolute metric error on a trial-by-trial basis during encoding and retrieval (ROI analysis).

Region	Hemisphere	Brodmann area	MNI coordinates			T values/z values of maxima (cluster size in number of voxels)
			X	Y	Z	
Encoding						
Hippocampus (posterior)	R	–	36	−22	−8	6.81/4.60 (7)
Parahippocampal gyrus	R	–	30	−26	−16	6.41/4.45 (35)
Parahippocampal gyrus	L	–	−28	−44	−8	5.11/3.88 (21)
Retrieval						
Striatum (putamen)	L	–	−30	6	0	6.48/4.48 (92)
Striatum (putamen)	R	–	24	6	0	5.69/4.15 (98)
Hippocampus	L	–	−22	−10	−18	5.60/4.11 (95)

Spatial coordinates, anatomical locations, and cluster size of the local maxima in the group analysis, showing significant activations ($P \leq 0.05$, corrected for multiple comparisons) for the parametric modulation with absolute metric error on trial-by-trial basis. For abbreviations, see Tables 1a and 1b.
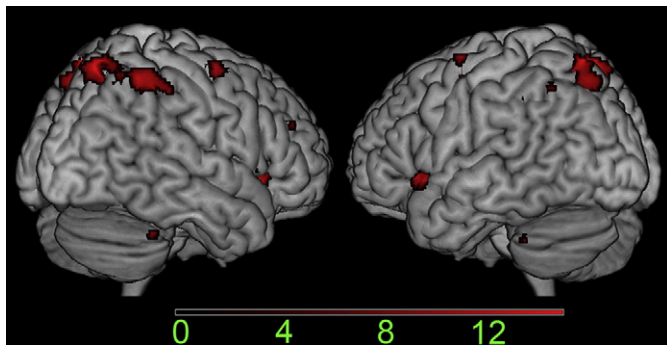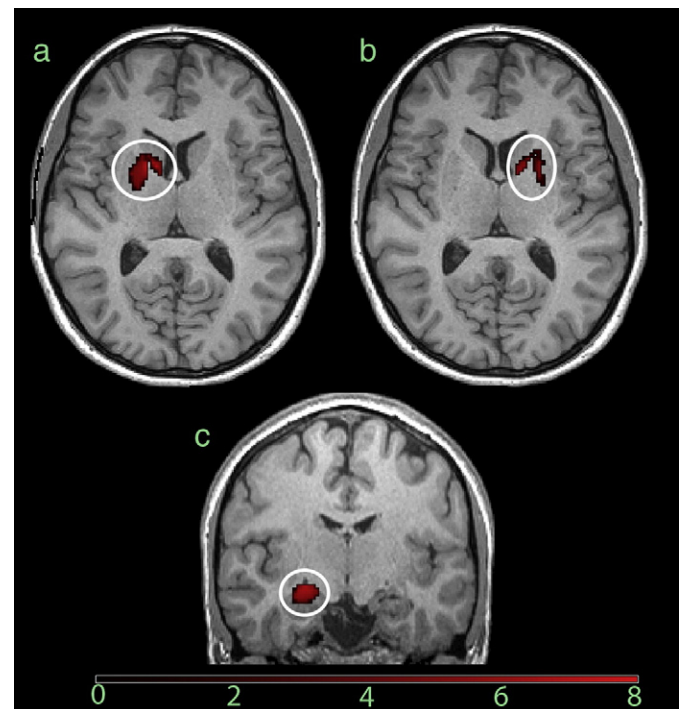
Fig. 6. Three-dimensional rendered MR images showing mean BOLD activity from the whole-brain analysis comparing good and poor navigators during the retrieval phase. *T* values are overlaid onto a rendered MNI-normalized template. Activated voxels buried within sulci are projected onto the cortical surface.

Ikeda and Osaka, 2007; Smith et al., 1995), as well as with spatial navigation and path integration (Doeller et al., 2008; Wolbers et al., 2007). However, the precise role of this frontal area remains elusive, since it is clearly involved in many other higher cognitive processes. The ROI analysis further revealed significantly stronger activity in the right parahippocampus for good versus poor navigators (Fig. 8c). The reverse comparison, testing for areas of greater activity in the poor navigators, revealed significant clusters only for the retrieval phase. During retrieval, the poor navigators showed significantly more activity in the left hippocampus (see Figs. 7c and 8d), the medial orbital frontal cortex and the cingulate (all based upon whole-brain analyses; see Table 3b). The medial prefrontal cortex and the cingulate are typically active when participants make decisions under uncertainty, especially under internally attributed uncertainty (Critchley et al., 2001; Volz et al., 2004). It is reasonable to assume that the poor navigators experienced greater uncertainty in their judgments relative to the good navigators.

Discussion

We measured brain activity with fMRI during object location learning, in which the encoding and retrieval stages of the task required participants to actively navigate within a virtual environment. Successful encoding of purely landmark-related knowledge, within a single trial and without reinforcement, was tightly linked to activity within the right hippocampus and the parahippocampus bilaterally. By contrast, the retrieval of relevant spatial representations during navigation to a remembered target was mediated by the striatum bilaterally and the left hippocampus. We also found large

Table 3a
Summary of fMRI findings for the analysis of good minus poor navigators (using a median split based on average absolute metric error) during encoding (whole-brain analysis).

Region	Hemisphere	Brodmann area	MNI coordinates			*T* values/*z* values of maxima (cluster size in number of voxels)
			X	Y	Z	
Good navigators>Poor navigators						
Precuneus/SPL	R	7	22	−54	56	8.04/4.93 (37)
MFG	L	6	−34	−2	56	7.27/4.69 (9)
CingG/MedFG	L	6/32	−2	12	48	6.86/4.55 (7)
SFG/MedFG	L	6	−8	2	58	6.79/4.52 (12)
Precuneus	R	7	10	−62	54	6.66/4.48 (7)

Spatial coordinates, anatomical locations, and cluster size of the local maxima in the group analysis, showing significant activations ($P \leq 0.05$, corrected for multiple comparisons) for the between-participants comparison, based on average metric errors during (a) the encoding phase and (b) the retrieval phase. For abbreviations, see Tables 1a and 1b.

Fig. 7. MR brain slices showing mean BOLD activity from the ROI analysis of good minus poor navigators during the retrieval phase. Good navigators showed stronger activity in two regions. (a) Left striatum (−14, 6, 10). (b) Right striatum (12, 4, 8). Poor navigators showed stronger activity in a single region. (c) Left hippocampus (−24, −12, −12).

differences in cortical activity between participants based on their behavioural performance. Good navigators showed greater activity in the medial and posterior parietal cortex during the encoding phase, and greater activity within parietal, frontal, striatal, and cerebellar regions during the retrieval phase relative to poor navigators.

Neural circuits underlying encoding of object location during navigation
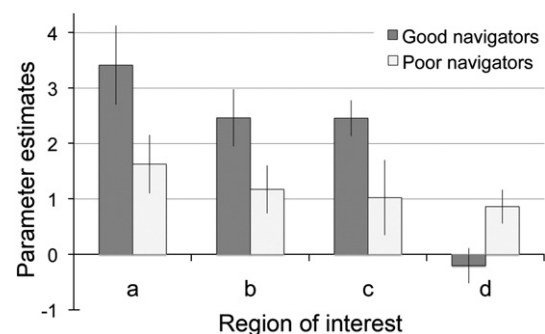
In our task, participants' viewpoint upon entering the arena changed between encoding and retrieval phases on 75% of the trials. Participants therefore had to form a flexible, allocentric representation of the spatial layout at encoding to ensure accurate target localization during the retrieval phase. Our finding that right hippocampal activity positively correlated with task performance during encoding is in line with previous studies which found that the right hippocampus is especially important whenever spatial associations need to be formed in a way that allows their flexible use (McNamara and Shelton, 2003; O'Keefe and Nadel, 1978).

Fig. 8. Parameter estimates (beta values, ±1 standard deviation) for the peak voxels from the ROI analysis of good minus poor navigators (separately for the two subgroups) during the retrieval phase. (a) Right striatum (12, 4, 8). (b) Left striatum (−14, 6, 10). (c) Right parahippocampus (30, −42, −8). (d) Left hippocampus (−24, −12, −12).

Table 3b
Summary of fMRI findings for the contrasts comparing good and poor navigators (using a median split based on average absolute metric error) during retrieval.

Region	Hemisphere	Brodmann area	MNI coordinates			T values/z values of maxima (cluster size in number of voxels)
			X	Y	Z	
Good navigators>Poor navigators						
Whole brain						
IPL/precuneus/SPL	R	7/40	10	−66	60	14.58/6.16 (531)
IFG/insula	L	47	−42	16	−6	13.17/5.94 (163)
Precuneus/SPL	L	7	−12	−68	64	12.58/5.84 (216)
MFG	R	6	32	−4	58	11.75/5.70 (163)
IFG/insula	R	47	36	22	−6	11.13/5.58 (200)
SFG/MFG	L/R	6/8	4	10	56	10.79/5.51 (180)
Precuneus	R	7/31	22	−68	34	9.57/5.24 (100)
IPL	L	40	−38	−40	40	9.48/5.22 (90)
Putamen	L	–	−16	6	8	8.26/4.90 (27)
MFG	L	6	−28	0	66	8.25/4.90 (73)
Cerebellum (anterior lobe)	R	–	40	−44	−34	7.58/4.70 (11)
Cerebellum (anterior lobe)	L	–	−34	−50	−36	7.26/4.60 (35)
Putamen	L	–	−20	10	0	7.22/4.59 (9)
Cerebellum (anterior lobe)	R	–	30	−58	−32	7.20/4.58 (17)
MFG	R	10	36	36	24	6.73/4.43 (14)
ROI						
Striatum (Caudate caudate and putamen)	R	–	12	4	8	5.70/4.03 (361)
Striatum (Caudate caudate and putamen)	L	–	−14	6	10	5.44/3.92 (390)
Parahippocampal gyrus	R	–	30	−42	−8	5.40/3.91 (26)
Poor navigators>Good navigators						
Whole brain						
MedFG	L/R	9	−2	52	28	10.20/5.38 (226)
PostCing	L/R	31	−4	−54	30	8.59/4.99 (53)
PostCing	R	31	8	−52	30	7.74/4.75 (11)
IFG/MFG	L	11/47	−32	36	−14	7.53/4.69 (8)
AntCing	R	32	10	26	−10	7.48/4.67 (25)
MedFG	L	10	−8	60	0	7.45/4.66 (42)
SFG	L	8	−12	34	54	7.11/4.55 (14)
ROI						
Hippocampus	L	–	−24	−12	−12	6.85/4.47 (157)

Spatial coordinates, anatomical locations, and cluster size of the local maxima in the group analysis, showing significant activations (P≤0.05, corrected for multiple comparisons) for the between-participants comparison, based on average metric errors during (a) the encoding phase and (b) the retrieval phase. For abbreviations, see Tables 1a and 1b.

We also found that activity within the left and right parahippocampal gyri during encoding was predictive of successful memory-guided navigation. Elevated parahippocampal activation could be indicative of the successful formation of mental representations of the virtual environment, which in turn leads to better task performance. Alternatively, elevated parahippocampal activation might mediate deeper processing of the scene-like landmark–target configurations, which then results in the successful formation of mental representations of the virtual environment in other brain areas like the hippocampus. The parahippocampus has a well-established role in scene processing; it is strongly activated when scenes are viewed or imagined, during active navigation (Aguirre et al., 1996; Maguire et al., 1998), as well as during passive viewing (Epstein and Kanwisher, 1998; Goh et al., 2004). Reports that topographical disorientation often arises after lesions of the right parahippocampal gyrus (Habib and Sirigu, 1987) also support the hypothesis that this region plays an important role in the acquisition and long-term storage of spatial memories (Rosenbaum et al., 2005; Teng and Squire, 1999).

Neural circuits underlying retrieval of object location during navigation

Successful retrieval was associated with increased activity in the striatum bilaterally and in the left hippocampus. During the retrieval phase, striatal activity was also significantly stronger in good versus poor navigators. By contrast, the poor navigators showed greater activity in the left hippocampus. The right hippocampus is often assumed to be especially important for spatial memory, whereas the left hippocampus is more involved in verbal, symbolic (Dolan and Fletcher, 1997; Trenerry et al., 1995), or context-dependent episodic memory (Burgess et al., 2002; Maguire et al., 1998). Contrary to

expectations, we did not observe any significant performance-related effects in the right hippocampus during the retrieval stage. Our finding that navigational ability was negatively correlated with participants' tendency to employ a verbal strategy suggests that the greater activity within the left hippocampal region in poor versus good navigators is due to the reliance by poor navigators on an inefficient, verbal strategy.

The increased striatal activity during retrieval suggests that landmark-based navigation within sparse environments, such as the one used in the current study, is determined by successful engagement of a non-declarative, perception-based spatial representation. It is widely accepted that the striatum is crucially involved in non-declarative or procedural memory processes (e.g., Poldrack et al., 2001). Moreover, animal and human studies have shown that procedural learning of responses to individual stimuli is mediated via the striatum (Doeller et al., 2008; Doeller and Burgess, 2008; Iaria et al., 2003; Packard and McGaugh, 1996). It might further be the case that, during the retrieval period, the striatum serves as a component of the neural representation of the goal and the procedural aspects of goal-directed behaviour (Hollerman et al., 2000). As such, the striatum might underlie the execution of appropriate goal-directed behaviour – or inhibition of inappropriate behaviour – in response to the remembered landmarks. The medial temporal lobe (i.e., hippocampus and parahippocampus) and basal ganglia (i.e., dorsal striatum) might function as independent memory systems, but may also interact or compete with each other (Poldrack and Packard, 2003). The observation of opposite trends in activation within the striatum and the hippocampus depending on participants' navigation performance suggests an inhibitory relationship between the two systems.

The role of the parietal cortex and cerebellum in active navigation

Areas within the medial and posterior parietal cortex were found to be significantly more active in good navigators than in poor navigators, during both encoding and retrieval. Subpopulations of neurons in the posterior parietal cortex respond to the positions of external stimuli relative to the retina, eye, head, trunk, and places or objects in the environment (Andersen and Buneo, 2002; Snyder et al., 1998). Based on such evidence, it has been suggested that the posterior parietal cortex translates directional information in cardinal coordinates into an egocentric direction signal necessary to guide movements to goal locations (Burgess et al., 2000). The more pronounced retrieval-related activity we observed in the good navigators might therefore reflect more efficient spatial updating within the posterior parietal cortex. Concurrent activation in parietal, striatal, and limbic regions might reflect cooperation between egocentric and allocentric coding strategies to solve 3D spatial tasks including navigation. This idea is consistent with recent models proposing such cooperation (Arbib, 1997; Burgess et al., 2002). Strong connections between the posterior parietal cortex, the hippocampal formation and the parahippocampal region (Seltzer and Pandya, 1984; Suzuki and Amaral, 1994) are further suggestive of functional interactions between these structures during spatial–cognition tasks such as orienting, navigating, and forming visuospatial memory traces.

We also found that the cerebellum was significantly more active during retrieval in the good versus poor navigators. Surprisingly, the cerebellum has not been closely examined previously in research on navigation, despite there being good evidence to link this brain structure with spatial behaviours in animals and humans. Significant cerebellar activity has been observed during tasks involving spatial orienting (Lee et al., 2005), exploratory behaviour (Petrosini et al., 1998; Pierce and Courchesne, 2001), mental rotation of objects (Molinari et al., 2004; Tagaris et al. 1998), and spatial working memory (Ronnberg et al., 2004; Smith et al., 2006). A possible mechanism by which the cerebellum could modulate spatial learning is via the cerebello-thalamo-cortical pathway, or via projections to ascending midbrain dopaminergic neurons. In support of this hypothesis, lesions of the ventrolateral–ventromedial nuclei of the thalamus, the main cerebellar efferent relay station to the cerebral cortex, cause place-learning deficits in the Morris Water Maze (Jeljeli et al., 2003). Moreover, the cerebellum is known to maintain reciprocal connections with the parietal cortex (Allen et al., 2005; Clower et al., 2001; Lynch and Tian, 2005). In our task, striatal, parietal, and cerebellar activity was significantly greater in the good versus poor navigators, consistent with the notion that these regions are part of a network supporting procedural aspects of memory-guided navigation, even in single-trial learning without reinforcement.

A limitation of our study is that we were not able to resolve dynamic patterns of functional relationship between key regions within the navigation network. In addition to our findings on the brain areas that are active during encoding and retrieval, it would be valuable to examine patterns of connectivity between these regions and to determine how functional connectivity changes with memory demands and behavioural performance. Another limitation of human fMRI studies in general is that they can only resolve activity patterns for large ensembles of neurons. To understand how individual neurons contribute to the processes underlying spatial navigation, it is necessary to employ microelectrodes to record single-unit activity (e.g., see Ekstrom et al., 2007). Unfortunately, such an approach in humans necessarily involves individuals with pre-existing neurological conditions (such as epilepsy), whose performance might not be representative of the normal population.

Summary

Our findings indicate that the right hippocampus and the parahippocampal gyrus bilaterally underlie successful memory encoding of object locations during active navigation, while the striatum bilaterally and the left hippocampus are important for memory retrieval. Stronger striatal activity in good navigators might reflect a procedural component of the learning and retrieval process that is predominantly active in good navigators, whereas stronger left hippocampal activity in less successful navigators might indicate use of a verbal or symbolic code by this group. Greater parietal activity in good navigators might indicate a more effective spatial updating process present in these individuals. For future studies, it will be important to further explore the involvement of aforementioned brain regions in spatial memory by varying the temporal attributes of the task, the size of the virtual environment, and the visual appearance and number of landmarks and targets.

References

Aguirre, G.K., Detre, J.A., Alsop, D.C., D'Esposito, M., 1996. The parahippocampus subserves topographical learning in man. Cereb. Cortex 6, 823–829.
Allen, G., McColl, R., Barnard, H., Ringe, W.K., Fleckenstein, J., Cullum, C.M., 2005. Magnetic resonance imaging of cerebellar–prefrontal and cerebellar–parietal functional connectivity. Neuroimage 28, 39–48.
Andersen, R.A., Buneo, C.A., 2002. Intentional maps in posterior parietal cortex. Annu. Rev. Neurosci. 25, 189–220.
Aminoff, E., Gronau, N., Bar, M., 2007. The parahippocampal cortex mediates spatial and nonspatial associations. Cereb. Cortex 17, 1493–1503.
Arbib, M.A., 1997. From visual affordances in monkey parietal cortex to hippocampo-parietal interactions underlying rat navigation. Philos. Trans. R. Soc. Lond., B. Biol. Sci. 352, 1429–1436.
Bohbot, V.D., Iaria, G., Petrides, M., 2004. Hippocampal function and spatial memory: evidence from functional neuroimaging in healthy participants and performance of patients with medial temporal lobe resections. Neuropsychology 18, 418–425.
Burgess, N., Jackson, A., Hartley, T., O'Keefe, J., 2000. Predictions derived from modelling the hippocampal role in navigation. Biol. Cybern. 83, 301–312.
Burgess, N., Maguire, E.A., O'Keefe, J., 2002. The human hippocampus and spatial and episodic memory. Neuron 35, 625–641.
Clower, D.M., West, R.A., Lynch, J.C., Strick, P.L., 2001. The inferior parietal lobule is the target of output from the superior colliculus, hippocampus, and cerebellum. J. Neurosci. 21, 6283–6291.
Courtney, S.M., Ungerleider, L.G., Keil, K., Haxby, J.V., 1997. Transient and sustained activity in a distributed neural system for human working memory. Nature 386, 608–611.
Critchley, H.D., Mathias, C.J., Dolan, R.J., 2001. Neural activity in the human brain relating to uncertainty and arousal during anticipation. Neuron 29, 537–545.
Doeller, C.F., Burgess, N., 2008. Distinct error-correcting and incidental learning of location relative to landmarks and boundaries. Proc. Natl. Acad. Sci. U. S. A. 105, 5909–5914.
Doeller, C.F., King, J.A., Burgess, N., 2008. Parallel striatal and hippocampal systems for landmarks and boundaries in spatial memory. Proc. Natl. Acad. Sci. U. S. A. 105, 5915–5920.
Dolan, R.J., Fletcher, P.C., 1997. Dissociating prefrontal and hippocampal function in episodic memory encoding. Nature 388, 582–585.
Ekstrom, A.D., Bookheimer, S.Y., 2007. Spatial and temporal episodic memory retrieval recruit dissociable functional networks in the human brain. Learn. Mem. 14, 645–654.
Ekstrom, A.D., Kahana, M.J., Caplan, J.B., Fields, T.A., Isham, E.A., Newman, E.L., Fried, I., 2003. Cellular networks underlying human spatial navigation. Nature 425, 184–188.
Ekstrom, A., Viskontas, I., Kahana, M., Jacobs, J., Upchurch, K., Bookheimer, S., Fried, I., 2007. Contrasting roles of neural firing rate and local field potentials in human memory. Hippocampus 17, 606–617.
Epstein, R.A., 2008. Parahippocampal and retrosplenial contributions to human spatial navigation. Trends Cogn. Sci. 10, 388–396.
Epstein, R.A., Higgins, T.S., Thompson-Schill, S.L., 2005. Learning places from views: variation in scene processing as a function of experience and navigational ability. J. Cogn. Neurosci. 17, 73–83.
Epstein, R.A., Kanwisher, N., 1998. A cortical representation of the local visual environment. Nature 392, 598–601.
Epstein, R.A., Parker, W.E., Feiler, A.M., 2007. Where am I now? Distinct roles for parahippocampal and retrosplenial cortices in place recognition. J. Neurosci. 27, 6141–6149.

Goh, J.O.S., Siong, S.C., Park, D., Gutchess, A., Hebrank, A., Chee, M.W.L., 2004. Cortical areas involved in object, background, and object–background processing revealed with functional magnetic resonance adaptation. J. Neurosci. 24, 10223–10228.

Grön, G., Wunderlich, A.P., Spitzer, M., Tomczak, R., Riepe, M.W., 2000. Brain activation during human navigation: gender-different neural networks as substrate of performance. Nat. Neurosci. 3, 404–408.

Habib, M., Sirigu, A., 1987. Pure topographical disorientation: a definition and anatomical basis. Cortex 23, 73–85.

Hartley, T., Maguire, E.A., Spiers, H.J., Burgess, N., 2003. The well-worn route and the path less travelled: distinct neural bases of route following and wayfinding in humans. Neuron 37, 877–888.

Hollerman, J.R., Tremblay, L., Schultz, W., 2000. Involvement of basal ganglia and orbitofrontal cortex in goal-directed behavior. Prog. Brain Res. 126, 193–215.

Iaria, G., Petrides, M., Dagher, A., Pike, B., Bohbot, V.D., 2003. Cognitive strategies dependent on the hippocampus and caudate nucleus in human navigation: variability and change with practice. J. Neurosci. 23, 5945–5952.

Ikeda, T., Osaka, N., 2007. How are colors memorized in working memory? A functional magnetic resonance imaging study. Neuroreport 18, 111–114.

Janzen, G., van Tourennout, M., 2004. Selective neural representation of objects relevant for navigation. Nat. Neurosci. 7, 673–677.

Janzen, G., Jansen, C., van Turennout, M., 2008. Memory consolidation of landmarks in good navigators. Hippocampus 18, 40–47.

Jeljeli, M., Strazielle, C., Caston, J., Lalonde, R., 2003. Effects of ventrolateral–ventromedial thalamic lesions on motor coordination and spatial orientation in rats. Neurosci. Res. 47, 309–316.

Lee, T.M.C., Liu, H.L., Hung, K.N., Pu, J., Ng, Y.B., Mak, A.K.Y., Gao, J.H., Chan, C.C.H., 2005. The cerebellum's involvement in the judgment of spatial orientation: a functional magnetic resonance imaging study. Neuropsychologia 43, 1870–1877.

Ludowig, E., Trautner, P., Kurthen, M., Schaller, C., Bien, C.G., Elger, C.E., Rosburg, T., 2008. Intracranially recorded memory-related potentials reveal higher posterior than anterior hippocampal involvement in verbal encoding and retrieval. J. Cogn. Neurosci. 20, 841–851.

Lynch, J.C., Tian, J.R., 2005. Cortico-cortical networks and cortico-subcortical loops for the higher control of eye movements. Prog. in Brain. Res. 151, 461–501.

Maguire, E.A., Burgess, N., Donnett, J.G., Frackowiak, R.S., Frith, C.D., O'Keefe, J., 1998. Knowing where and getting there: a human navigation network. Science 280, 921–924.

McNamara, T.P., Shelton, A.L., 2003. Cognitive maps and the hippocampus. Trends Cogn. Sci. 7, 333–335.

Molinari, M., Petrosini, L., Misciagna, S., Leggio, M.G., 2004. Visuospatial abilities in cerebellar disorders. J. Neurol. Neurosurg. Psychiatry 75, 235–240.

O'Keefe, J., Nadel, L., 1978. The Hippocampus as a Cognitive Map. Oxford, Oxford UP.

Orban, P., Rauchs, G., Balteau, E., Degueldre, C., Luxen, A., Maquet, P., Peigneux, P., 2006. Sleep after spatial learning promotes covert reorganization of brain activity. Proc. Natl. Acad. Sci. U. S. A. 103, 7124–7129.

Packard, M.G., McGaugh, J.L., 1996. Inactivation of hippocampus or caudate nucleus with lidocaine differentially affects expression of place and response learning. Neurobiol. Learn. Mem. 65, 65–72.

Petrosini, L., Leggio, M.G., Molinari, M., 1998. The cerebellum in the spatial problem solving: a co-star or a guest star? Progr. Neurobiol. 56, 191–210.

Pierce, K., Courchesne, E., 2001. Evidence for a cerebellar role in reduced exploration and stereotyped behavior in autism. Biol. Psychiatry 49, 655–664.

Poldrack, R.A., Packard, M.G., 2003. Competition among multiple memory systems: converging evidence from animal and human brain studies. Neuropsychologia 41, 245–251.

Poldrack, R.A., Clark, J., Pare-Blagoev, E.J., Shohamy, D., Cresco Moyano, J., Myers, C., Gluck, M.A., 2001. Interactive memory systems in the human brain. Nature 414, 546–550.

Richardson, A.E., Montello, D.R., Hegarty, M., 1999. Spatial knowledge acquisition from maps and from navigation in real and virtual environments. Mem. Cogn. 27, 741–750.

Ronnberg, J., Rudner, M., Ingvar, M., 2004. Neural correlates of working memory for sign language. Cognit. Brain Res. 20, 165–182.

Rosenbaum, R.S., Gao, F., Richards, B., Black, S.E., Moscovitch, M., 2005. "Where to?" remote memory for spatial relations and landmark identity in former taxi drivers with Alzheimer's disease and encephalitis. J. Cogn. Neurosci. 17, 446–462.

Ruddle, R.A., Payne, S.J., Jones, D.M., 1997. Navigating buildings in 'desk-top' virtual environments: experimental investigations using extended navigational experience. J. Exp. Psychol.: Appl. 3, 143–159.

Schacter, D.L., Wagner, A.D., 1999. Medial temporal lobe activations in fMRI and PET studies of episodic encoding and retrieval. Hippocampus 9, 7–24.

Seltzer, B., Pandya, D.N., 1984. Further observations on parieto-temporal connections in the rhesus monkey. Exp. Brain Res. 55, 301–312.

Smith, A.M., Fried, P.A., Hogan, M.J., Cameron, I., 2006. Effects of prenatal marijuana on visuospatial working memory: an fMRI study in young adults. Neurotoxicol. Teratol. 28, 286–295.

Smith, E.E., Jonides, J., Koeppe, R.A., Awh, E., Schumacher, E.H., Minoshima, S., 1995. Spatial versus object working memory: PET investigations. J. Cogn. Neurosci. 7, 337–356.

Snyder, L.H., Grieve, K.L., Brotchie, P., Andersen, R.A., 1998. Separate body- and world-referenced representations of visual space in parietal cortex. Nature 394, 887–891.

Suzuki, W.A., Amaral, D.G., 1994. Perirhinal and parahippocampal cortices of the macaque monkey: cortical afferents. J. Comp. Neurol. 350, 497–533.

Tagaris, G.A., Richter, W., Kim, S.G., Pellizzer, G., Andersen, P., Ugurbil, K., Georgopoulos, A.P., 1998. Functional magnetic resonance imaging of mental rotation and memory scanning: a multidimensional scaling analysis of brain activation patterns. Brain Res. Rev. 26, 106–112.

Teng, E., Squire, L.R., 1999. Memory for places learned long ago is intact after hippocampal damage. Nature 400, 675–677.

Trenerry, M.R., Jack Jr., C.R., Cascino, G.D., Sharbrough, F.W., Ivnik, R.J., 1995. Gender differences in post-temporal lobectomy verbal memory and relationships between MRI hippocampal volumes and preoperative verbal memory. Epilepsy Res. 20, 69–76.

Tzourio-Mazoyer, N., Landeau, B., Papathanassiou, D., Crivello, F., Etard, O., Delcroix, N., Mazoyer, B., Joliot, M., 2002. Automated anatomical labeling of activations in SPM using a macroscopic anatomical parcellation of the MNI MRI single subject brain. NeuroImage 15, 273–289.

Volz, K.G., Schubotz, R.I., von Cramon, D.Y., 2004. Why am I unsure? Internal and external attributions of uncertainty dissociated by fMRI. NeuroImage 21, 848–857.

Weiskopf, N., Hutton, C., Josephs, O., Deichmann, R., 2006. Optimal EPI parameters for reduction of susceptibility-induced BOLD sensitivity losses: a wholebrain analysis at 3 T and 1.5 T. Neuroimage 33, 493–504.

Wolbers, T., Wiener, J.M., Mallot, H.A., Büchel, C., 2007. Differential recruitment of the hippocampus, medial prefrontal cortex, and the human motion complex during path integration in humans. J. Neurosci. 27, 9408–9416.